METALS AND MATERIALS International, Vol. 14, No. 6 (2008), pp. 729~738
doi: 10.3365/met.mat.2008.12.729 Published 18 December 2008

Influence of Co Content on the Biocompatibility and Bio-Corrosion of Super Ferritic Stainless Steels

Y. R. Yoo[1], S. G. Jang[2], H. S. Nam[2], G. T. Shim[2], H. H. Cho[3], J. G. Kim[4], and Y. S. Kim[2,*]

[1]Center for Advanced Life Cycle Engineering, University of Maryland,
College Park, MD 20742, USA
[2]The Center of Green Materials Technology, School of Advanced Materials Engineering,
Andong National University,
388, Songcheon-dong, Andong-si, Gyeongbuk 760-749, Korea
[3]Chosun Welding Co. ltd,
865 Jangheung-dong, Nam-gu, Pohang-si, Gyeongbuk 790-240, Korea
[4]School of Advanced Materials Science and Engineering, Sungkyunkwan University,
300, Cheoncheon-dong, Jangan-gu, Suwon-si, Gyeonggi 440-746, Korea

Bio-metals require high corrosion resistance, because their biocompatibility is closely related to this parameter. Bio-metals release metal ions into the human body, leading to deleterious effects. Allergies, dermatitis, and asthma are the predominant systemic effects resulting in the human body. In particular, Ni is one of the most common causes of allergic contact dermatitis. In the present work, we designed new ferritic stainless steels wherein Ni is replaced with Co under consideration of allergic respondes and microstructural stability. This work focuses on the effect of Co content on the biocompatibility and corrosion resistance of high PRE super ferritic stainless steels in bio-solution and acidic chloride solution. In the case of the acidic chloride solution, with increasing Co content in the ferritic stainless steels, passive current density increased and critical pitting temperature (CPT) decreased. Also, in the passive state, AC impedance and repassivation rate were reduced. These results are attributed to the thermodynamic stability of cobalt ions, as indicated in the E-pH diagram for a Co-H2O system. However, in the case of bio-solutions, with increasing Co content of the alloys, the passive current density decreased. AC impedance and repassivation rate meanwhile increased in the passive state. This is due to the increased ratios of $Cr_2O_3/Cr(OH)_3$ and [Metal Oxide]/[Metal + Metal Oxide] of the passive film formed in bio-solution.

Key words: super ferritic stainless steel, passive film, PRE, cobalt, cytotoxicity

1. INTRODUCTION

Biomaterials designed for commercial use can be classified into four kinds of materials: metallic, ceramic, polymeric, and composite materials. Among these materials, metallic biomaterials have been used as implants in the form of bone plates, bone screws, hip joints, dental implants, guide wires, stents, *etc*. [1]. Because metallic biomaterials contact the body directly or indirectly, biocompatibility is very important for their application. The biocompatibility of metallic biomaterials is closely related to their corrosion resistance. Specifically, metallic ions formed by an electrochemical process can induce cytotoxicity by ingress to their tissues. In addition to the above considerations, mechanical properties such as high tensile strength, elongation, and low elastic coefficient are necessary as well as ease of manufacture and formability [2,3].

Bio-metals include stainless steels, Ti and its alloys, Co-Cr alloys, Ni-Ti alloys, Ni-Cr alloys, and so on. Initially, bone screws and bone plates were made from stainless steels and Co-Cr alloys were also used as they are associated with low inflammation in the body. Ti alloys also show good biocompatibility and have recently been used. However, the applicability of Ti alloys is restricted when repeated motion and vibration are concerns, since they show low strength and wear resistance. Also, because of their low strength and poor formability, Ti alloys have found limited application to the head area. On the other hand, 316 L stainless steels release metallic ions owing to low corrosion resistance in the body. In particular, Ni is one of the most common causes of allergic contact dermatitis [4-6]. To address this problem, Ni-substitution for cobalt can reduce the allergies in the body and

*Corresponding author: yikim@andong.ac.kr

Ni-free super ferritic stainless steel can minimize the dissolution of metallic ions as it offers high corrosion resistance [7-9].

Since Co is an austenite stabilizer, Co has a similar effect regarding microstructural stability to that of nickel [10]. According to the E-pH diagram for a Co-H_2O system [11], oxides such as CoO_2 and $Co(OH)_3$ can form thermodynamically. Also, it is well known that Co can reduce the precipitation rate of intermetallic compounds including sigma phase when sensitizing [12]. In vitro studies have indicated that particulate Co is toxic to human osteoblast-like cell lines and inhibits synthesis of type-I collagen, osteocalcin, and alkaline phosphatase in culture media. However, particulate Cr and CoCr alloys are well tolerated by cell lines and have no significant toxicity [13-15].

Super stainless steels have good corrosion resistance, thereby minimizing the dissolution of metallic elements by corrosion in the body. Cr, Mo, and W in stainless steels can form a stable passive film on the surface and thus they show a similar corrosion resistance to Ti and its alloys. Moreover, super stainless steels show superior mechanical properties and formability over Ti and its alloys.

In the present work, four Ni-free super ferritic stainless steels were produced and their Co content was controlled from 0 % to 12 %. The effect of Co content on the biocompatibility and bio-corrosion of ferritic stainless steels has also been investigated.

2. EXPERIMENTAL PROCEDURES

2.1. Materials

The stainless steels evaluated in this study were prepared from commercially pure grade Fe, Cr, Co, Mo, W, Fe-Si, and Fe-Mn. Melting was carried out in a high frequency vacuum induction furnace. After casting, only the solid sections of the ingot were taken to prepare the test specimens. These sections were first soaked for 1 hour per 1-inch of thickness and hot rolled to a thickness of 6 mm. The hot rolled specimens were pickled in a mixed solution containing 10 % HNO_3 and 3 %HF at 66 °C to remove the hot working scale. They were subsequently cold rolled to 1.0 mm, annealed at 1050 °C for 30 min, and then water quenched. A small section was cut from each sample and used for a chemical analysis. Table 1 shows the chemical compositions of the experimental alloys. Figure 1 shows the phase diagram of the experimental alloys plotted by ThermoCalc and the crystal structure of the 4 alloys was shown to be ferritic.

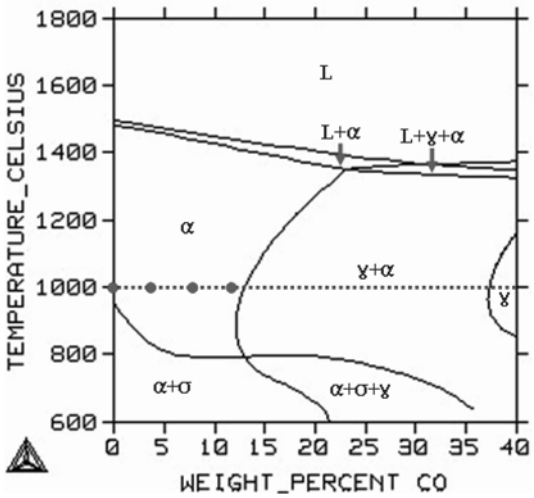

Fig. 1. Phase diagram of the experimental alloys plotted by ThermoCalc™.

2.2. Cytotoxicity test

Specimens were prepared for each material for use in a cytotoxicity test. They were processed such that a surface area of 1 cm^2 came into contact with agar; the surfaces were sterilized with ethylene oxide gas and cleansed with distilled water for sterilization. Gutta Percha was used as a positive control and glass as a negative control. L-929 cells, mouse fibroblast cell-lines, were cultivated in α-MEM medium and the produced supernatant solution was used for the cytotoxicity test. A sample of the supernatant solution (10 ml) in α-MEM medium was added to a Petri dish and cultivated for 24 h. The α-MEM medium was then removed, and 10 ml of Eagle's agar medium at 45 °C to 50 °C was added to each Petri dish and left to stand at room temperature for 30 min. After the Eagle's agar medium had solidified, neutral red vital stain solution (10 ml) was added slowly to the center of the dish and allowed to spread over the surface for 30 min. Immediately after removing the dyeing solution, the specimens were placed in contact with the agar and incubated for 24 h in a 37 °C, 5 % CO incubator. First, the Petri dish was placed on top of a white paper, and then the zone index was measured after observing the size of the discolored area. The lysis index was measured by calculating the lysed ratio of the

Table 1. Chemical composition of the experimental alloys(wt.%)

Alloys	Cr	Mo	W	Mn	Si	C	Co	N	Fe	PRE
SFCo1	22.5	3.4	4.4	0.44	0.29	0.024	0.17	0.0029	bal.	41.1
SFCo2	22.3	3.5	4.6	0.47	0.38	0.036	4.16	0.0027	bal.	41.5
SFCo3	22.3	3.3	4.4	0.46	0.28	0.024	8.15	0.0017	bal.	40.5
SFCo4	22.5	3.5	4.5	0.44	0.09	0.034	12.1	0.0025	bal.	41.6

*PRE = %Cr + 3.3(%Mo + 0.5%W) + 30%N

cells in the discolored area with an inverted phase contrast microscope (CK2, Olympus, Japan). Finally, the response index was measured by averaging the zone and Lysis indices of the four specimens [16].

2.3. *In vitro* metal ion release testing

In vitro metal ion release testing was performed upon each of three specimens, which were inserted into a Teflon specimen holder. The area exposed to the solution was 1 cm^2. Each specimen was immersed in a separate screw-topped glass bottle containing 100 ml of Hanks' balanced salt solution, and the bottles were stored in an incubator at 37 °C in ambient air containing 5 % CO_2. After the specimens were immersed for 10 days, 5 ml of the solution was removed from each bottle and analyzed for Fe, Cr, and Mo by graphite furnace atomic adsorption spectroscopy (AAS, Model Spectra 220FS, Varian) and for Co and W by ICP (Inductively Coupled Plasma Spectrometer, Model Flame Modula S, Spectra(Germany)).

2.4. Polarization test

The experimental alloys were subjected to anodic polarization in 0.5 N HCl + 1 N NaCl (Acidic chloride solution) at 50 °C, and Hanks' balanced salt solution (HBSS) at 37 °C [17] and an artificial saliva solution [18] using a Potentiostat (Gamry DC105). The specimen was polished to #600 using SiC paper. The solutions were deaerated by purging them with pre-purified nitrogen gas for 30 min at a rate of 90 ml/min. prior to immersion of the specimen. After immersion, a cathodic potential of −200 mV, which exceeds the corrosion potential, was applied to the specimen for 10 min. The Specimenwas then maintained for 10 minutes at an open circuit potential, and then polarized anodically from its corrosion potential at a scanning rate of 1 mV/min. A saturated calomel electrode (SCE) was used as a reference electrode and high-density graphite rods as a counter electrode.

2.5. CPT and CCT measurements

The critical pitting temperature and critical crevice temperature were measured by the method described in ASTM G48-00 [19]. The test solution was 6 % $FeCl_3$ + 1% HCl and the specimen was polished to #600 using SiC paper. The starting temperature was based on ASTM G48-00 and the specimen was immersed for 24 h at each temperature.

2.6. XPS analysis

X-ray photoelectron spectroscopy (XPS, PHI 5700 ESCA, Perkin-Elmer) was used to analyze the chemical species and chemical state of the passive film. The films were formed by subjecting the specimen to anodic polarization from the corrosion potential to the passive potential: +100 mV (SCE) for 600 s at 25 °C and 3600 s at 37 °C, respectively, in acidic chloride solution and HBSS. All of the XPS measurements were performed with the use of Al-Kα excitation (BE; 1,486.6 eV) and an analyzer pass energy of 23.5 eV for high-resolution scans. The take-off angle was 75. All of the spectra were compensated by charge shifting the carbon spectrum to adventitious carbon at 284.6 eV. The spectra were resolved into their components after iterative background subtraction according to the Shirley fitting procedure and curve fitting with the Gaussian-Lorentzian formula. The binding energies of some of the chemical species in the XPS analysis are available in the literature [17,20].

2.7. AC impedance measurement

The AC impedance was measured for the passivated surface. The passive film was formed for 1 h at +100 mV (SCE). Impedance spectra were obtained in Hanks' balanced salt solution at 37 °C and acidic chloride solution at 50 °C. The amplitude of the applied AC potential was 50 mV and the impedance was measured from 0.01 Hz to 10 kHz at the passive potential.

2.8. Repassivation Rate Test

A repassivation rate test was conducted in 50 °C, 0.5 N HCl + 1 N NaCl and 37 °C Hanks' balanced salt solution using a potentiostat (Gamry DC 105). The specimen was reduced for 20 min by cathodic polarization at -1000 mV(SCE) in 0.5 N HCl + 1 N NaCl and in Hanks' balanced salt solution. A passivation potential (+600 mV(SCE)) was then applied and, from the obtained current-time curve, the repassivation index was calculated [21].

3. RESULTS AND DISCUSSION

3.1. Effect of cobalt content on the biocompatibility and bio-corrosion of super ferritic stainless steels

Biocompatibility was evaluated on the bases of the results of the cytotoxicity test and ions release test. Table 2 shows the effect of cobalt content on the cytotoxicity of super ferritic stainless steels. The commercial alloy 316 L stainless steel was mildly cytotoxic but the experimental alloys were non-cytotoxic regardless of cobalt content. Figure 2 shows the effect of cobalt content on the release of metallic ions from super ferritic stainless steels in 37 °C, Hanks' balanced salt solution. The immersion time was 10 days. Release of iron and tungsten ions was high among several elements. With increased Co content, the total ion release was slightly reduced. From the above results, the effect of Co content on the biocompatibility could not be differentiated, because the experimental alloys have high corrosion resistance, with a PRE value greater than 40.

Figure 3 shows the effect of Co content on the anodic polarization behavior of the experimental alloys and a commercial alloy, 316 L stainless steel, in deaerated 37 °C, Hanks' balanced salt solution. After cathodic polarization for 10 min

Table 2. Effect of cobalt contents on the cytotoxicity of super ferritic stainless steels

Samples	Decolorization index	Lysis index	Response index	Cytotoxicity
SFCo1	0	0	0/0	none(-)
	0	0	0/0	none(-)
SFCo2	0	0	0/0	none(-)
	0	0	0/0	none(-)
SFCo3	0	0	0/0	none(-)
	0	0	0/0	none(-)
SFCo4	0	0	0/0	none(-)
	0	0	0/0	none(-)
316L	0~1	1~1	0/1	Mildly cytotoxic
	0~1	1~1	0/1	Mildly cytotoxic
Positive(Gutta Percha)	3	4	3/4	moderate(++)
Negative(glass)	0	0	0/0	none(-)

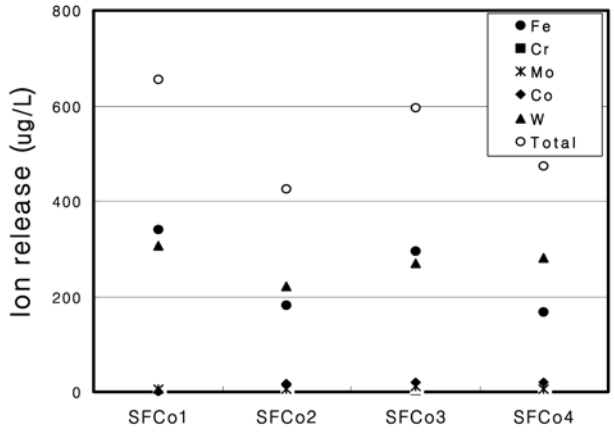

Fig. 2. Effect of Co contents on ion release in Hanks' balanced salt solution at 37 °C (10 days immersion).

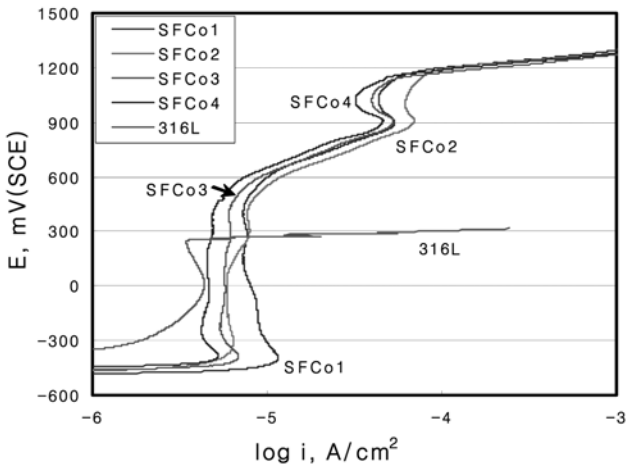

Fig. 3. Effect of Co contents on anodic polarization behavior of the experimental alloys in Hanks' balanced salt solution at 37 °C.

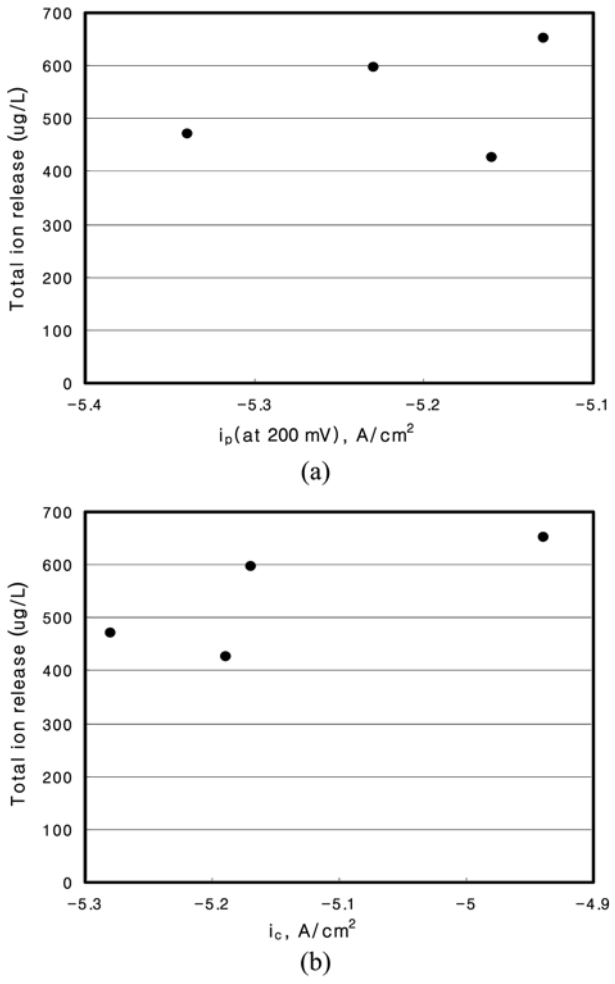

Fig. 4. Relationship between total ion release (10 days immersion) and (a) passive current density, i_p, (b) critical passive current density, i_c in Hanks' balanced salt solution at 37 °C.

at ER-200 mV and then for 10 min at open circuit potential, the specimen was anodically polarized from the corrosion potential. The corrosion potential of 316 L alloy was higher than that of the experimental alloys, but pitting was initiated near +300 mV(SCE) and the alloy was severely corroded. The corrosion potential of the experimental alloys was relatively low since the alloys do not contain nickel. With increasing Co content, the corrosion potential increased slightly, and the passive current density and critical passive current

density decreased. Above +1000 mV (SCE), the current density abruptly increased; however, this was due to the oxygen evolution rather than corrosion.

Figure 4 shows the relationship between total ion release and passive current density, ip, and critical passive current density, ic, in 37 °C, Hanks' balanced salt solution. The results were obtained from Figs. 2 and 3. As shown in the figures, with increasing passive current density, *i.e.* decreasing the Co content in the alloys, the total ion release increased. Also, the total ion release increased by increasing the critical current density, *i.e.* decreasing the Co content in the alloys. Figure 5 shows the relationship between the repassivation index and passive current density, ip, and the critical passive current density, ic, in 37 °C, Hanks' balanced salt solution. With decreasing passive current density, *i.e.* increasing the Co content in the alloys, the repassivation index increased. Also, with decreasing critical passive current density, *i.e.* increasing the Co content in the alloys, the repassivation index increased.

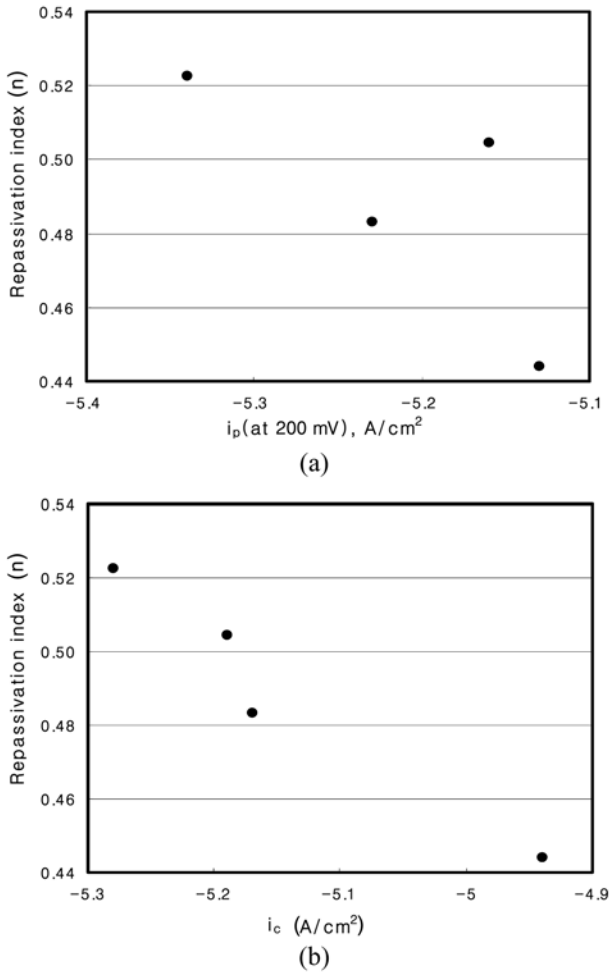

Fig. 5. Relationship between repassivation index and (a) passive current density, i_p, (b) critical passive current density, i_c in Hanks' balanced salt solution at 37 °C.

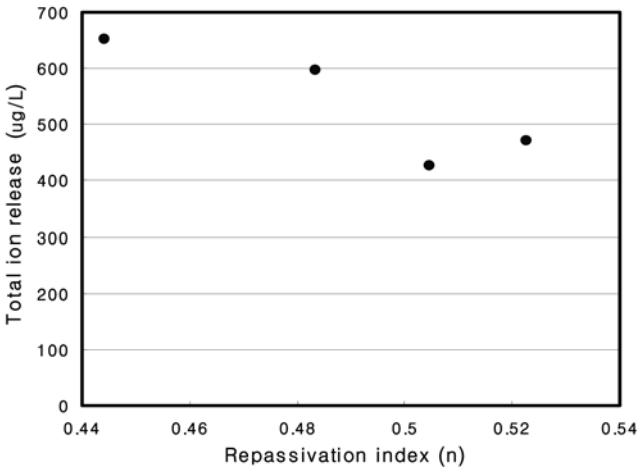

Fig. 6. Relationship between total ion release (10 days immersion) and repassivation index in Hanks' balanced salt solution at 37 °C.

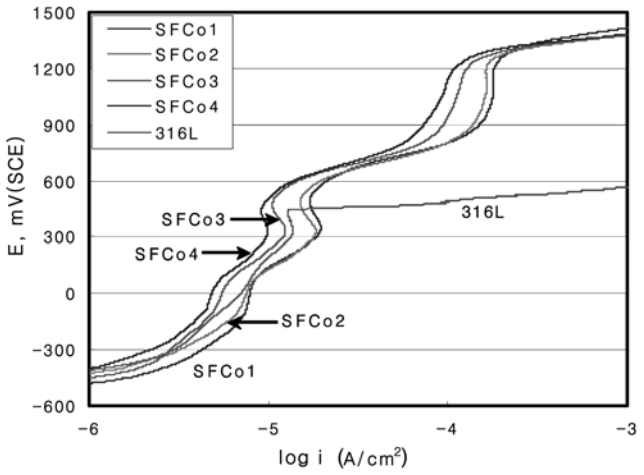

Fig. 7. Effect of Co contents on anodic polarization behavior of the experimental alloys in artificial saliva solution at 37 °C.

Figure 6 shows the relationship between total ion release and repassivation index in 37 °C, Hanks' balanced salt solution. As the repassivation index was increased, the total ion release also decreased. When the Co content in the alloys was increased, the repassivation rate increased and thus suppressed the dissolution of metal elements.

Figure 7 shows the effect of Co content on anodic polarization behavior of the experimental alloys and commercial alloy, 316 L stainless steel, in a deaerated 37 °C, artificial saliva solution. After cathodic polarization for 10 min at ER-200 mV and then for 10 min at open circuit potential, the speciemen was anodically polarized from the corrosion potential. The corrosion potential of 316 L alloy was higher than that of the experimental alloys, but pitting was initiated near +450 mV(SCE) and the alloy was severely corroded. The corrosion potential of the experimental alloys was relatively low, since the alloys do not contain nickel. With increasing Co content, the corrosion potential slightly increased,

and the passive current density decreased. Above +1200 mV (SCE), the current density abruptly increased, but this was due to the oxygen evolution rather than corrosion.

On the basis of the above results, it is thus determined that cobalt is beneficial for the bio-corrosion resistance of super ferritic stainless steel.

3.2. Passivation mechanism in acidic chloride solution and bio-solutions

Figure 8 shows the CPT and CCT of the experimental alloys. Figure 8(a) shows the CPT values of SFCo1 (75 °C), SFCo2 and SFCo3 (70 °C), and SFCo4 (65 °C). The four alloys have the same PRE value and thus cobalt reduced the critical pitting temperature. That is, with increasing cobalt content in the alloys, the pitting corrosion resistance was decreased. Figure 8(b) shows the CCT values of SFCo1 (45 °C), SFCo2 and SFCo3 (40 °C), and SFCo4 (35 °C). On average, the CCT was about 30 °C lower than the CPT. Corresponding with the CPT results, cobalt reduced the critical crevice temperature. That is, with increasing cobalt content in the alloys, the crevice corrosion resistance was decreased.

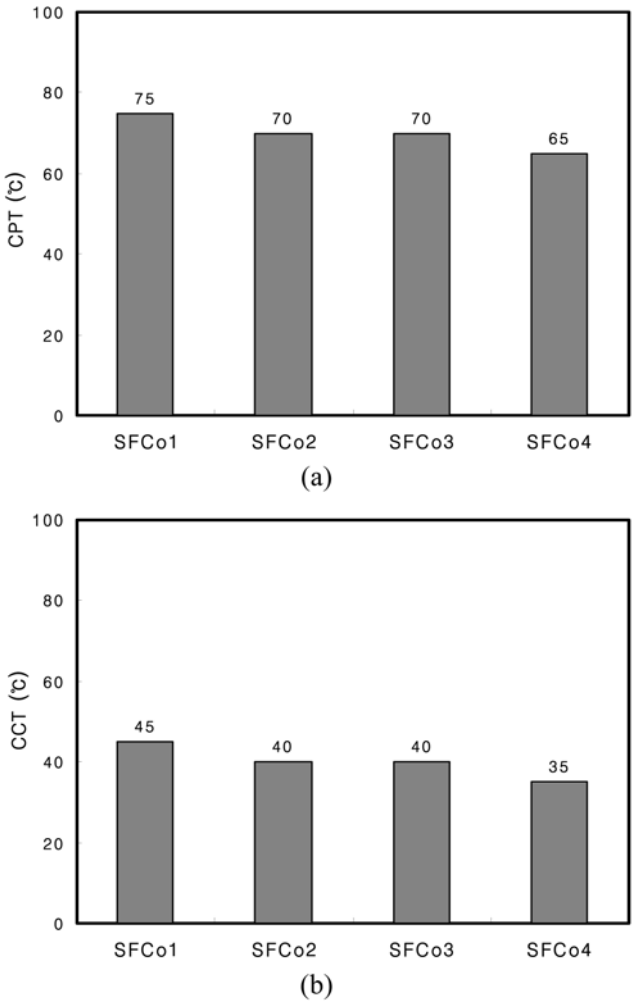

Fig. 8. Effect of Co contents on (a) critical pitting temperature and (b) critical crevice temperature of the experimental alloys evaluated by ASTM G48-00.

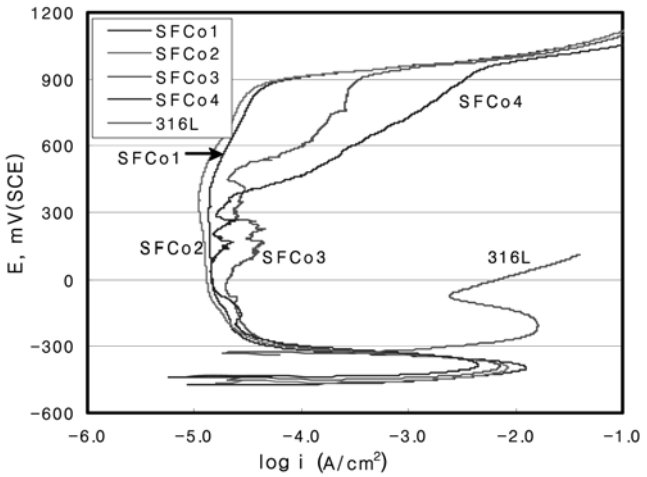

Fig. 9. Anodic polarization curves of the experimental alloys in 0.5 N HCl + 1N NaCl solution at 50 °C.

Figure 9 presents anodic polarization curves of the experimental alloys in deaerated 50 °C, 0.5 N HCl + 1 N NaCl solution at a scanning rate of 1 mV/s. After cathodic polarization for 10 minutes at ER-200 mV and then for 10 min at open circuit potential, the specimen was anodically polarized from the corrosion potential. The corrosion potential of 316L stainless steel was higher than that of the experimental alloys due to its Ni content and the 316L alloy did not form passivity and was severely corroded. However, the experimental alloys formed good passivity. With increasing Co content in the alloys, the corrosion potential increased and the critical passive current density decreased. However, the passive current density increased and the transpassive potential decreased

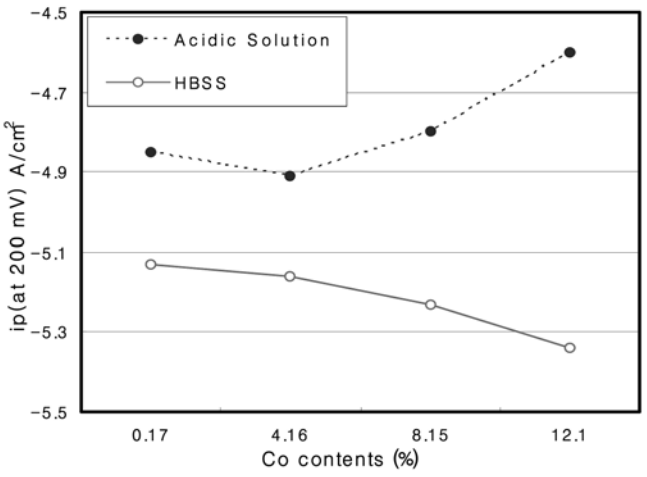

Fig. 10. Effect of Co contents on the passive current density at + 200 mV (SCE) in 50 °C, 0.5N HCl + 1N NaCl and 37 °C, Hanks' balanced salt solution.

when the Co content was increased. This behavior is similar in trend with the results of CPT and CCT, but is contrary to the results in bio-solutions.

Figure 10 shows the effect of Co content on the passive current density at +200 mV (SCE) in 50 °C, 0.5 N HCl + 1 N NaCl and 37 °C, Hanks' balanced salt solution. When an increase of Co content, the passive current density decreased in the Hanks' balanced salt solution, but increased in the acidic salt solution. This indicates that the effect of Co was dependent upon the corrosion environment, *e.g.* ionic species. It has previously been reported that even when alloys had high PRE values and Ni content, the critical passive current density in a bio-solution was increased and this behavior was closely related to the presence of EDTA in the bio solutions [17].

As discussed above, Co in the alloys improves the corrosion resistance in bio-solutions but reduces it in acidic salt solution. In order to find the origin of this behavior, an XPS analysis was performed on the passive film, which is critical to the corrosion resistance of stainless steels.

Figure 11 shows the chemical states of the main elements in the passive film of SFCo3 formed in 50 °C, 0.5N HCl + 1N NaCl as determined by a XPS analysis (Take off angle 75°); (a) is for Fe, (b) is for Cr, (c) is for Mo, and (d) is for W. The formation potential was+100 mV (SCE) and was applied for 600 s. As shown in the figures, the Fe peak was comprised of Fe^{M}, Fe^{2+}, and Fe^{3+}, the Cr peak consisted of Cr^{M}, Cr_2O_3, $Cr(OH)_3$, and CrO_4^{2-}, the Mo peak consisted of Mo^{M}, MoO_2, $MoO(OH)_2$, and MoO_4^{2-}, and the W peak consisted of W^{M}, WO_2, WO_3, and WO_4^{2-}.

Figure 12 shows the chemical states of the main elements in the passive film of SFCo3 formed in 37 °C, Hanks' bal-

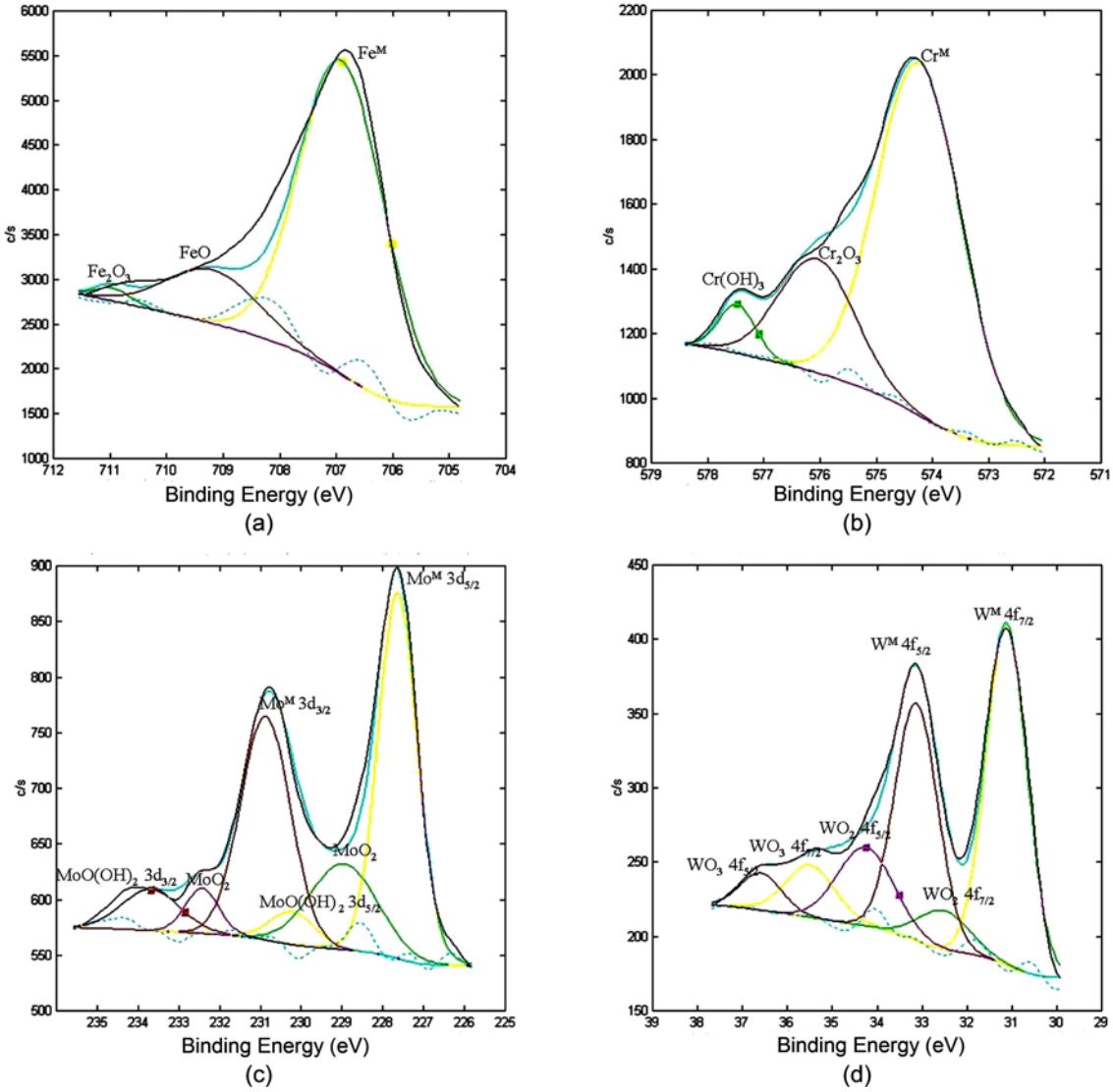

Fig. 11. Chemical states of main elements consisting of the passive film of SFCo3 formed in 50 °C, 0.5N HCl + 1N NaCl by XPS analysis (Take off angle = 75°) ; (a) Fe, (b) Cr, (c) Mo, and (d) W.

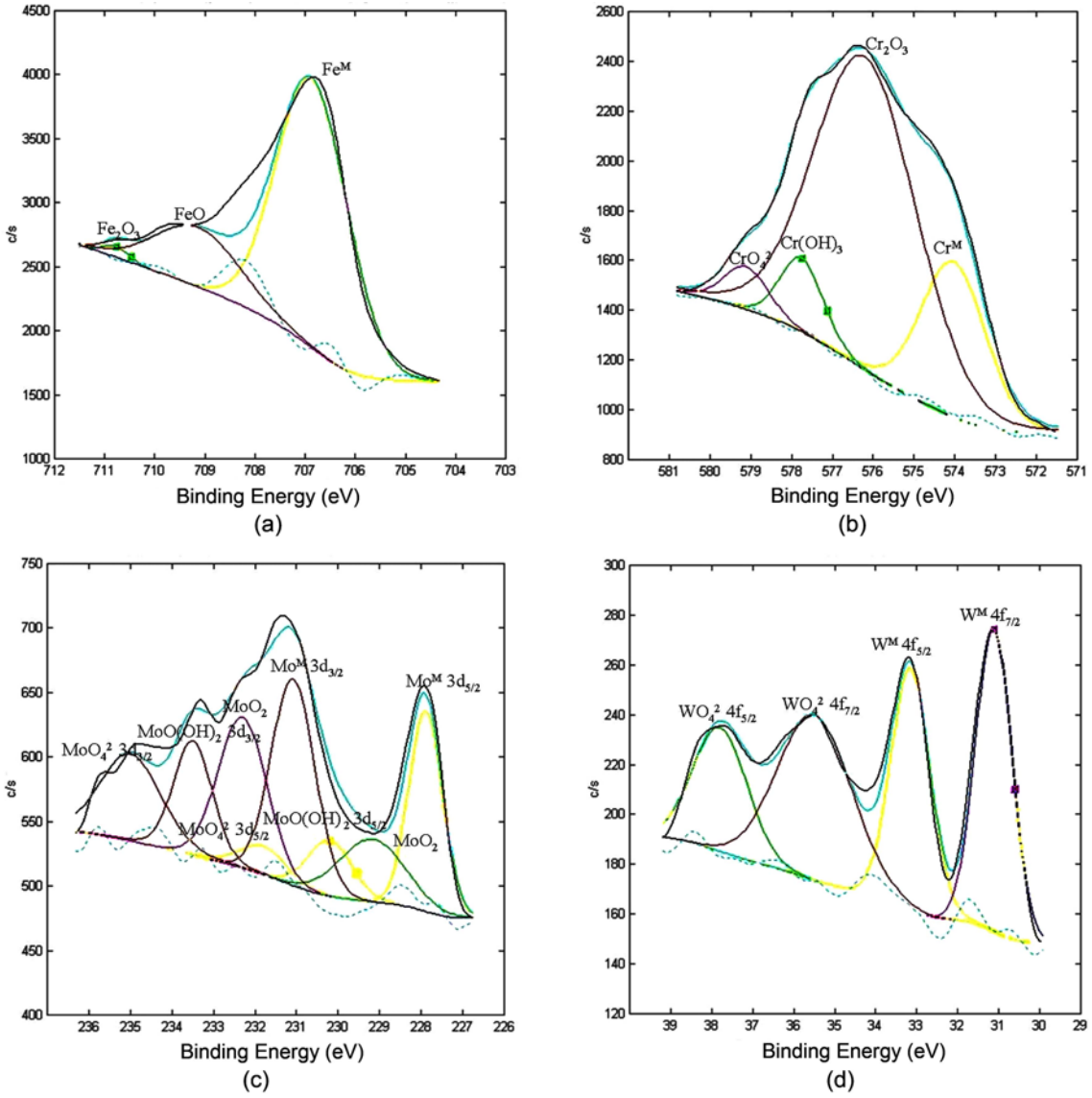

Fig. 12. Chemical states of main elements consisting of the passive film of SFCo3 formed in Hanks' balanced salt solution at 37 by XPS analysis (Take off angle = 75°) ; (a) Fe, (b) Cr, (c) Mo, and (d) W.

anced salt solution as determined by a XPS analysis (Take off angle 75°); (a) is for Fe, (b) is for Cr, (c) is for Mo, and (d) is for W. The formation potential was +100 mV(SCE) and was applied for 3600 s. As shown in the figures, the chemical states of Fe, Cr, Mo, W were the same as those in 50 °C, 0.5 N HCl + 1 N NaCl.

Figure 13 reveals the effect of Co content on the ratios of [Metal Oxide] / [Metal + Metal Oxide] of each element of the passive films formed in (a) 37 °C, Hanks' balanced salt solution, (b) 50 °C, 0.5 N HCl + 1 N NaCl solution, and (c) the total ratio between two solutions. In Hanks' balanced salt solution, with increasing Co content in the alloys, the ratio of [Metal Oxide] / [Metal + Metal Oxide] excluding tungsten increased. However, in the acidic chloride solution, with increasing Co content in the alloys, the ratio of [Metal Oxide] / [Metal + Metal Oxide] excluding molybdenum decreased. Furthermore, as shown in Fig. 13(c), with increasing Co content in the alloys, the ratio of [Metal Oxide] / [Metal + Metal Oxide] of all elements increased in the case of the Hanks' balanced salt solution but decreased in the case of the acidic chloride solution. According to the E-pH diagram for a Co-H_2O system, cobalt can corrode to cobalt ions in low pH solutions [11]. Figure 14 reveals the effect of Co content on the ratios of Cr_2O_3 / $Cr(OH)_3$ of the passive films formed in 50 °C, 0.5 N HCl + 1 N NaCl and 37 °C, Hanks' balanced salt solutions. It is well known that this ratio is a very important factor with respect to the corrosion resistance of stainless steels [22-26]. As shown in Figure 14, with increasing Co content in the alloys, the ratio of Cr_2O_3 / $Cr(OH)_3$ increased in the case of the Hanks' balanced salt solution but decreased

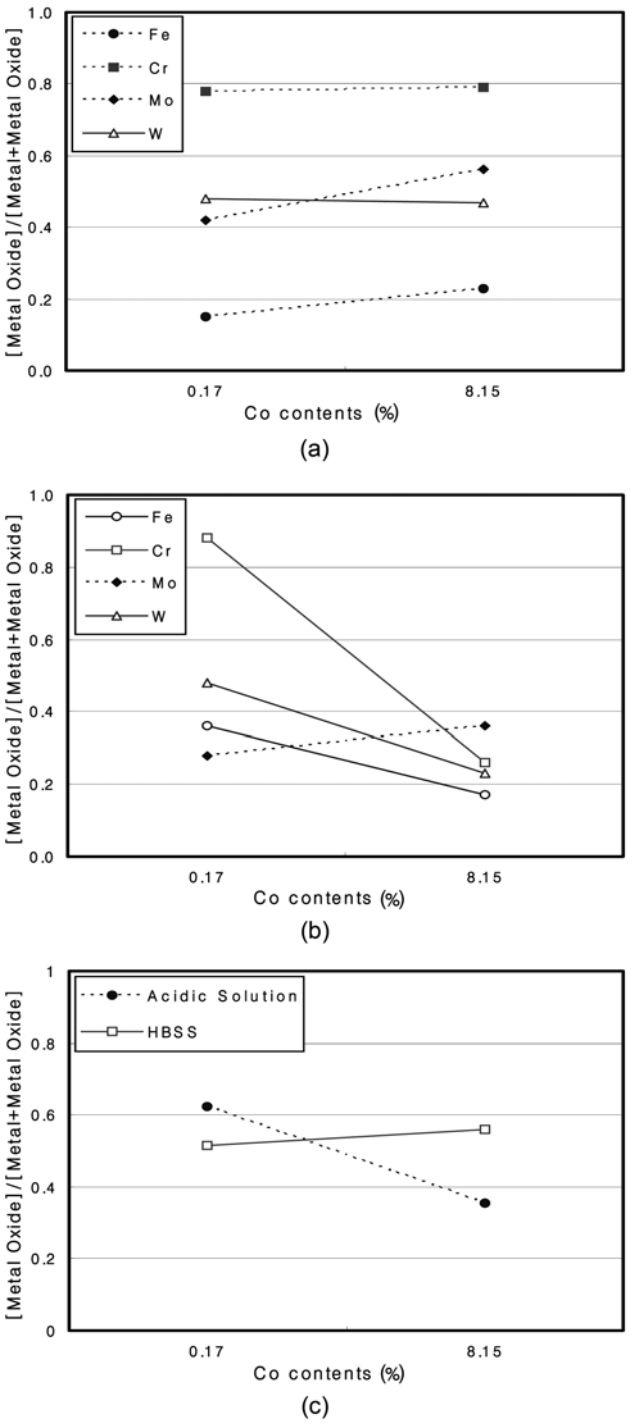

Fig. 13. Effect of Co contents on the ratios of [Metal Oxide] / [Metal + Metal Oxide] of each element of the passive films formed in (a) Hanks' balanced salt solution at 37 °C, (b) 0.5 N HCl + 1 N NaCl solution at 50 °C and (c) total ratio between two solutions.

in the case of the acidic chloride solution.

Figure 15 presents the effect of Co content on the repassivation index in 50 °C, 0.5 N HCl + 1 N NaCl and 37 °C, Hanks' balanced salt solution. A high repassivation index indicates

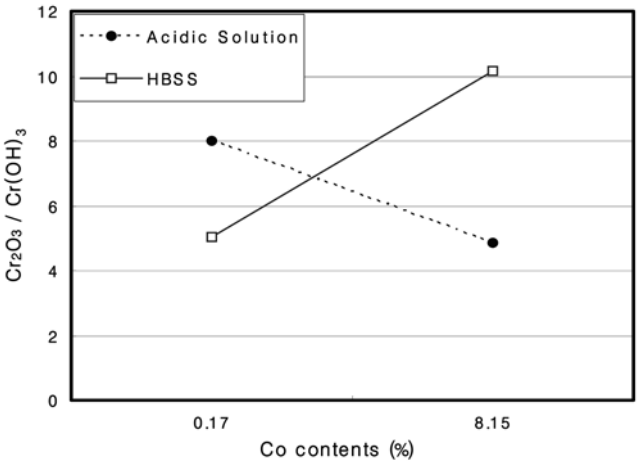

Fig. 14. Effect of Co contents on the ratios of $Cr_2O_3/Cr(OH)_3$ obtained by XPS analysis for the passive films formed in 50 °C, 0.5N HCl + 1N NaCl and 37 °C, Hanks' balanced salt solutions.

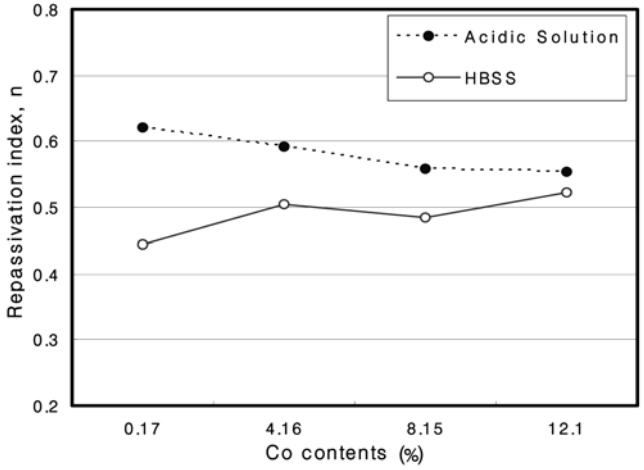

Fig. 15. Effect of Co contents on the repassivation indices obtained by repassivation tests in 50 °C, 0.5N HCl + 1N NaCl and 37 °C, Hanks' balanced salt solution.

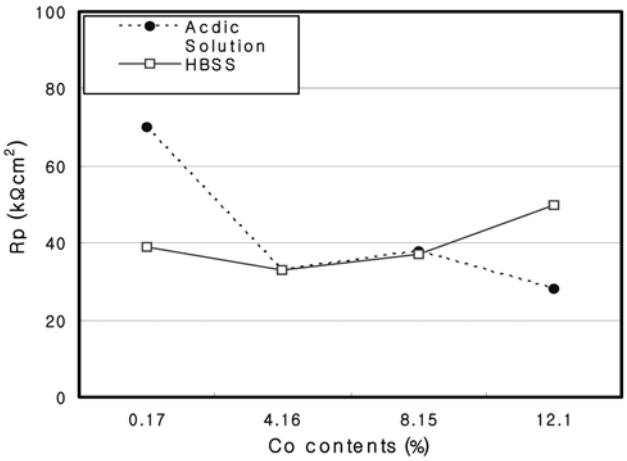

Fig. 16. Effect of Co contents on the resistance obtained by AC impedance measurements for the passive film formed in 50 °C, 0.5N HCl + 1N NaCl and 37 °C, Hanks' balanced salt solution.

that the repassivation rate is fast. As shown in the figure, with increasing Co content in the alloys, the repassivation index increased in the Hanks' balanced salt solution, but decreased in the acidic chloride solution. Figure 16 shows the effect of Co content on the resistance of the passive film formed in 50 °C, 0.5 N HCl + 1 N NaCl and 37 °C, Hanks' balanced salt solution. The resistance of the passive film was obtained by AC impedance measurements. The resistance of the film in the case of the Hanks' balanced salt solution gradually increased when the Co content was increased. However, the resistance of the film in the case of the acidic chloride solution decreased substantially when the Co content was increased.

4. CONCLUSIONS

(1) Four super ferritic stainless steels showed non-cytotoxicity regardless of Co content, because the alloys have high PRE values over 40. In vitro metal ion release testing revealed that the total ion release decreased when the Co content in the alloys was increased.

(2) In an acidic chloride solution, Co content in the alloys decreased the CPT and CCT and reduced the repassivation rate and the resistance of the passive film. These results are attributed to the thermodynamical stability of cobalt ions, as indicated in the E-pH diagram for a Co-H_2O system.

(3) However, in a bio-solution, with increased Co content in the alloys, the passive current density and critical passive current density decreased, and the repassivation rate and the resistance of the passive film increased. This is due to the increased ratios of Cr_2O_3 / $Cr(OH)_3$ and [Metal Oxide] / [Metal + Metal Oxide] of the passive film formed in a bio-solution.

ACKNOWLEDGMENT

This research was supported by the Program (KB-05-1-007) for the Training of Graduate Student in Regional Innovation conducted by the Ministry of Commerce, Industry and Energy of the Korean Government.

REFERENCES

1. Y. G. Kim, *J. Kor. Inst. Electric. Electron. Mater. Eng.* **15**, 18 (2002).
2. K. A. Gross and C. C. Berndt, *2nd Plasma-Technik Symposium*, **3**, 159 (1991).
3. G. T. Oh, Y. S. Kim, and G. N. Kim, *Met. Mater. -Int.* **42**, 64 (2004).
4. J. Black and G. Hastings, *Handbook of Biomaterial Properties,* Chapman & Hall, New York (1998).
5. B. D. Ratner, A. S. Hoffman, F. J. Schoen, and J. E. Lemons, *Biomaterials Science An Introduction to Materials in Medicine,* Academic Press, San Diego (1997).
6. J. A. Helsen and H. J. Breme, *Metals as Biomaterials,* John Wiley & Sons Ltd., West Sussex (1998).
7. P. Haudrechy, B. Mantout, and A. Frappax, *Contact Dermatitis* **37**, 113 (1997).
8. J. R. Fisher and G. A. Rosenblum, *J. Am. Med. Assoc.* **248**, 1065 (1982).
9. J. K. Bass, H. Fine and G. J. Cisneros, *Am. J. Orthod. Dentofac. Orthop.* **103**, 280 (1993).
10. J. Beddoes and J. Gordon Parr, *Introduction to Stainless Steels*, ASM International, Materials Park, OH, USA (1999).
11. M. Pourbaix, *Atlas of Electrochemical Equilibria*, NACE, Houston, Texas, USA (1974).
12. A. Yoshitake, A. Kuhara, and T. Ishii, Ferritic-Austenitic Duplex Stainless Steel, *United States Patent Number 5,238,508* (1990).
13. J. B. Park and J. D. Bronzino, *Biomaterials, Principles and Applications*, CRC Press (2003).
14. D. F. Williams, "*Biocompatibitilty in Clinical Practice*", CRC Press (1982).
15. D. Granchi, G. Ciapetti, L. Savarino, D. Cavendagna, M. E. Donati and A. Pizzoferrato, *J. Biomed. Mater. Res.* **31**, 183 (1996).
16. ISO 7405:1997(E), "*Dentistry-Preclinical Evaluation of Biocompatibility of Medical Devices used in Dentistry - Test Methods for Dental Materials*", ISO (1997).
17. Y. R. Yoo, S. G. Jang, K. T. Oh, J. G. Kim, and Y. S. Kim, *J. Biomed. Mater. Res. B* **86**, 310 (2008).
18. K. T. Oh, Y. S. Kim, Y. S. Park, and K. N. Kim, *J. Biomed. Mater. Res. B* **69**, 183 (2004).
19. ASTM G48-00, *Standard Test Methods for Pitting and Crevice Corrosion Resistance of Stainless Steels and Related Alloys by Use of Ferric Chloride Solution*, ASTM (2000).
20. XPS Database Systems, *XPS & AES Software & XPS Spectra Handbooks,* http://www.xpsdata.com (2007).
21. F. P. Ford, *Corrosion* **52**, 375 (1996).
22. Y. S. Kim, *Met. Mater. -Int.* **4**, 183 (1998).
23. Y. S. Kim, Y. S. Park, B. Mitton, and R. Latanision, *Proc. Symposium on Critical Factors in Localized Corrosion III* (eds., R. G. Kelly, G. S. Frankel, P. M. Natishan, and R. C. Newman), p. 89, The Electrochemical Society, USA (1999).
24. Y. S. Kim, Y. S. Park, *J. Corros. Sci. Soc. Kor* **18**, 97 (1989).
25. C. R. Clayton, C. R. Clayton, and Y. C. Lu. *J. Electrochem. Soc.* **133**, 2465 (1986).
26. K. S. Kim, H. Y. Chang, and Y. S. Kim, *Corros. Sci. Tech.* **2**, 75 (2003).